Sputtered Zinc Oxide Films for Silicon Thin Film Solar Cells: Material Properties and Surface Texture

Oliver Kluth,
Bernd Rech,
Heribert Wagner
Forschungszentrum Jülich (IPV)
O.Kluth@fz-juelich.de

Texture etching of sputtered ZnO:Al films has opened up a variety of possibilities to design optimised light trapping schemes for silicon thin film solar cells. A comprehensive material study on sputtered ZnO:Al was performed focusing on the relationship between film growth, structural properties and the surface morphology obtained after wet chemical etching. These results served as basis for the development of a modified Thornton growth model for sputtered ZnO:Al films on glass substrates.

Moreover, these studies are also necessary to provide additional experimental background for theoretical work on light scattering and light trapping as well as to support the up-scaling of texture-etched ZnO to large areas and its implementation in solar modules. To evaluate the suitability of the light scattering properties, the light trapping of differently textured glass/ZnO substrates was studied directly in silicon thin film solar cells. ZnO:Al substrates with adapted surface texture for different applications and reduced absorption losses contributed to the development of µc-Si:H p-i-n and a-Si:H/µc-Si:H stacked p-i-n cells with cell efficiencies of 9 % and 11.3 % (stabilized), respectively.

ZnO:Al films were prepared with different sputter techniques (rf, dc) from ceramic ZnO:Al_2O_3- and metallic Zn:Al-targets using a wide range of deposition parameters on bare glass substrates. The sputter parameters deposition pressure and substrate temperature were found to have the major influence on the ZnO:Al material properties. With both rf and dc sputter deposition technique highly conductive and transparent ZnO:Al films were prepared applying low sputter pressures. In case of the reactive dc sputter mode using metallic targets, substrate temperatures above 200 °C were required to achieve high transparencies.

A characteristic increase in the specific resistance was observed, if the deposition pressure exceeded a certain value, typical for each deposition technique and parameter regime *(see Fig. 1)*.

Figure 1

Pressure dependence of the specific resistance ρ for rf- and dc-sputtered ZnO:Al films. The films were sputtered from ceramic $ZnO:Al_2O_3$-targets at T_S =150 °C and 270 °C.

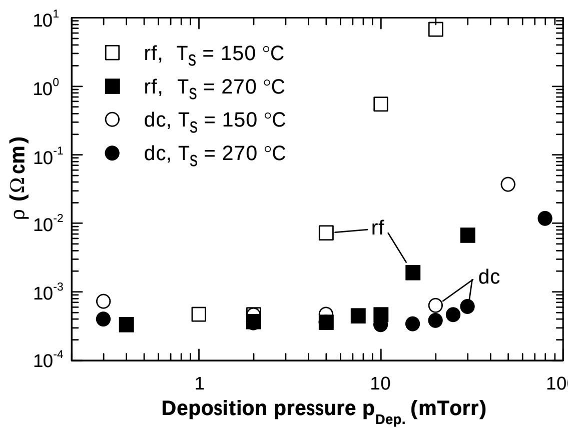

To obtain textured surfaces the ZnO:Al films were etched in diluted hydrochloric acid (HCl). The corresponding surface morphologies were characterised by Atomic Force Microscopy (AFM) and Scanning Electron Microscopy (SEM) measurements. Even for similar optical and electrical film properties, the ZnO films show distinctly different surface structures after the etching step. Again the deposition pressure has the main influence as it controls the structural properties of the initial films and hence the resulting surface structure after etching. In low pressure regimes craters of characteristic distribution, lateral size and depth arise at the surface due to anisotropic etching. Increasing the deposition pressure results in reduced opening angles and greater depth of the craters *(see Table I)*.

$P_{Dep.}$ (mTorr)	appearance	δ_{rms} (nm)	α (°C)	etch rate (nm/s)
0.4	craters	33	131	5.1
2	craters	64	125	5.1
5	craters	40	136	5.8
10	craters/hills	42	132	4.6
15	hills	76	73	18.3
30	hills	79	47	21

Table 1

Root mean square roughness δ_{rms} and opening angle α of rf-sputtered ZnO:Al films on glass found after 15 s of etching in 0.5 % HCl (see text).

The correlation of sputter parameters, film growth and structural properties can be under-stood in terms of a modified Thornton model *(see Fig. 2)*. The Thornton model was developed to describe the growth of sputtered metals as a function of two parameters, substrate temperature and sputter pressure.

Since there are some fundamental differences between TCO material and metals we suggest some modifications of the original Thornton model to make it applicable to rf-sputtered ZnO:Al films on glass substrates. First, we have to take into account that ZnO exhibits a distinctly higher melting point T_M=1975 °C than typical metals. Therefore, in the modified Thorton model the substrate temperature T_S is taken into account instead of the normalised value T_S/T_M. Furthermore, our experimental results underline that in contradiction to sputtered metal films, for sputtered ZnO:Al the substrate temperature plays a less important

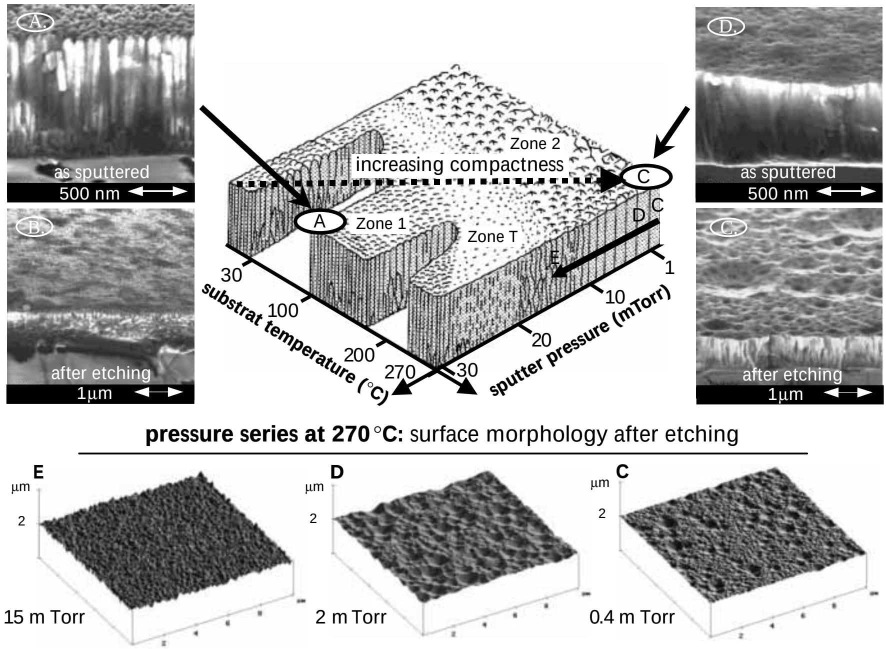

Figure 2

The modified Thornton model describes the correlation between sputter parameters (sputter pressure and substrate temperature), structural film properties and etching behaviour of rf-sputtered ZnO:Al films on glass substrates. The pressure series at T_S = 270 °C shows the systematic influence of the sputter pressure on the surface morphology after etching (see text).

role than the sputter pressure. Therefore, the pressure axis has been exchanged with the substrate temperature axis.

Fig. 2 shows the modified Thornton model, which is in good agreement with our experimental results. Note that due to the high melting point of ZnO Zone 3, typical for re-crystallisation, appears at much higher substrate temperatures. Zone 3 is therefore not present in the applied temperature range. The general statement of the original Thornton model is maintained: in-creasing the substrate temperature and reducing the sputter pressure leads to a more compact and dense film structure.

The bandwidth of structural variations is demonstrated by the example of two ZnO:Al samples, which have been deposited in two extremely different regimes. Sample A was deposited with a high sputter pressure of 30 mTorr and without intentional heating, while sample C was sputtered with the lowest possible pressure 0.3 mTorr and T_S=270 °C. The High-Resolution Scanning Electron Microscopy (HRSEM) images show the cross-section and the surface morphology of the films before and after etching. Sample A can be identified as a Zone 1 film with typical low compactness. The highly dense film structure of sample C can be found at the edge of Zone 2. In addition, the HRSEM-pictures of the etched samples show the distinctly different surface morphology. While sample A is only reduced in thickness with a fast etching rate maintaining a relatively smooth surface sample C is etched in an anisotropic process with small rate.

The AFM plots in *Fig. 3* show the systematic influence of the sputter pressure on the surface morphology of rf-sputtered ZnO:Al films after 15 s of etching in 0.5 % HCl. For extremely low pressure, craters of irregular lateral size and depth arise at the surface due to anisotropic etching at low etching rates. Increasing the deposition pressure results in more regularly dis-tributed craters of greater depth. Exceeding a certain transition pressure leads to considerably increased etching rates and a regular hill-like surface structure with significantly smaller feature sizes and opening angles.

The remarkable improvement in quantum efficiency obtained by the introduction of an ZnO:Al film with suitable surface texture and reduced absorption losses is nicely illustrated by the following example.

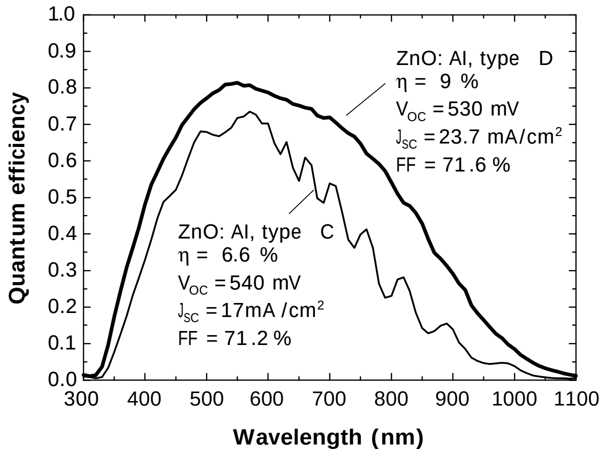

Figure 3
Quantum efficiency of two µc-Si:H pin solar cells co-deposited on ZnO:Al films of type C and D as shown in Fig. 2.

Textured ZnO films with type C and type D surface morphology *(see Fig. 2)* were applied in a µc-Si p-i-n solar cell with an i-layer thickness of 1.5 µm. In addition, the red/infrared transparency of the type D ZnO:Al was improved to reduce absorption losses.

Fig. 3 shows the QE curves of these two co-deposited cells. Smaller overall QE is obtained on the type C ZnO film with a less regular surface texture and a smaller rms-roughness com-pared to type D. A J_{sc} gain of more than 6 mA/cm^2 and 9 % efficiency are achieved due to the excellent light trapping and transparency of the type D ZnO:Al film. A-Si/µc-Si tandem cells deposited on optimised ZnO substrates yield an stabilized efficiency of 11.3 % with FF = 70 %, V_{oc} = 1.42 V and J_{sc} = 11.4 mA/cm^2 for a cell area of 1cm^2.